Optical refractivity of a pulsed plasma: Influence of the nonelectronic species

Ma. I. de la Rosa García, Ma. C. Pérez García, A. M. de Frutos Baraja, and S. Mar Sardaña
Universidad de Valladolid, Departamento de Física Aplicada III, Facultad de Ciencias, 47071 Valladolid, Spain
(Received 7 March 1990)

We present in this work refractivity measurements of very high accuracy and reliability in a helium pulsed plasma. The aim of this work is to determine the validity of the approximation based on the assumption that the contribution to the refractivity of the nonelectronic species is constant with wavelength. This approximation is used broadly to obtain the electronic density from refractivity at two wavelengths. Using this method, we have measured five wavelengths to determine this contribution.

INTRODUCTION

In characterizing a plasma, there are some parameters of very great significance. One of them is the electronic density. This parameter can be determined by both spectroscopic and interferometric methods. The interferometric measurements give a higher accuracy,[1] and they are based on the total refractivity of the plasma under study.

The refractivity of a low-density plasma can be expressed[2] as a sum of the refractivities of each of the present species in all their different ionization states:

$$(n-1)_e=-\frac{e^2N_e\lambda^2}{2\pi mc^2}\ ,$$

$$(n-1)_a=\frac{e^2}{2\pi mc^2}\sum_{\substack{i,j\\ i\neq j}}\frac{f_{ik}\lambda^2\lambda_{ik}^2N_i}{\lambda^2-\lambda_{ik}^2}\ ,$$

where e refers to free electrons and a to the ionization degree of each one of the plasma species, f refers to the oscillator strengths, N to the population density, λ is the working wavelength, and λ_{ik} is the wavelength of each transition.

Among the different species present in the plasma, the free electrons have the most important contribution to the plasma refractivity. This contribution strongly depends on the tuned wavelength of the interferometer. In contrast, the contribution of the rest of the species weakly depends on the wavelength. For this reason, most authors think that it is not necessary to do the complicated addition mentioned above. In fact, if we assume that the dependence of the nonelectronic species is constant, it is possible to determine the electronic density by measurements of the refractivity at two wavelengths.[3] Furthermore, it is standard in the literature to obtain the electronic density from measurements at only one wavelength, assuming that the contribution of the nonelectronic species is not only constant, but also very small.

We present here measurements of the refractivity of a helium pulsed plasma at several wavelengths with very high accuracy and reliability. These measurements allow us to obtain not only a very accurate electronic density but also the refractivity of the nonelectronic species in two different ways. The first is from a theoretical model broadly accepted, and the second consists of the natural extension of the common technique of measurement at two wavelengths, that is, the fitting of a function like

$$n-1=a\lambda^2+b\ .$$

In this way, we were able to analyze the accuracy of the electronic density obtained from measurements at one or two wavelengths and the dispersion due to nonelectronic species.

EXPERIMENTAL ARRANGEMENT AND MEASUREMENTS

Our plasma is formed from helium inside a lamp working with continuous flow, under the following conditions: pressure 11 mbar, flux 21 cm^3/min, electrical discharge 9.2 kV.

Under these conditions, we have done interferometric and spectroscopic measurements. In Fig. 1 the experimental setup is shown. The interferometer is likely the Twyman-Green,[4] with two mirrors M1 and M2 and the beam splitter BS1. The wavelengths used are 467.5, 488.0, 496.5, and 514.5 nm from an Ar laser, and 632.8 mn from a He-Ne one. The lens L does its work in the spectroscopic arrangement in order to correct for autoabsorption of the spectral lines, forming the image of the lamp center onto itself. To avoid this lens modifying the collimation of the beam in the interferometric arrangement, it is necessary that its focus lies on the mirror M1.

On the exit arm of the interferometer, a second plate BS2 splits the spectroscopic and the interferometric channels, deviating the latter to a microscope objective (MO) that focuses the light onto the entrance slit of a monochromator tuned to the working wavelength, in order to avoid lamp flash as much as possible. A photomultiplier situated near the exit slit detects the signal, which is recorded by a digital oscilloscope that finally sends the data to a computer. The temporal resolution in these measurements has been equal to 0.2 μs. The obtained interferometric pattern must be corrected from the arc

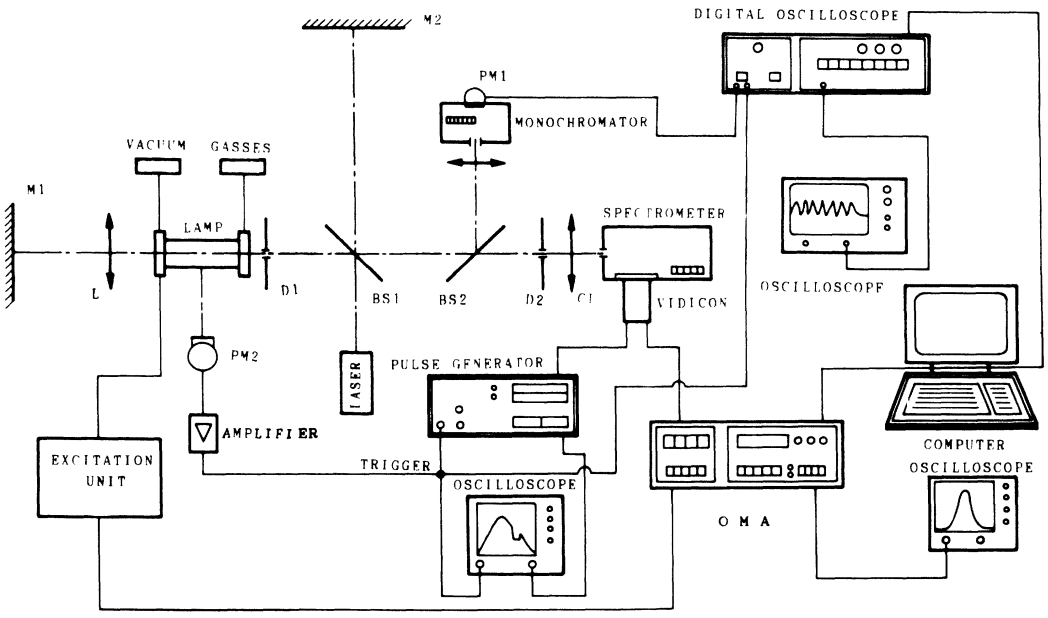

FIG. 1. Experimental arrangement.

emission in the spectral bandpass of the monochromator. All of the experimental apparatus was placed on an antivibratory table designed *ad hoc*.

We have also done spectroscopic measurements in order to determine the plasma temperature. The diaphragms D1 and D2 select a narrow and centered light beam, approximately homogeneous, which is focused by a cylindrical lens CL onto the entrance slit of a Jovin-Yvon spectrometer. Finally, the spectrum is detected with a vidicon and sent to an optical multichannel analyzer (OMA). We polarized the vidicon with the help of a high-voltage pulse generator, in which the delay, amplitude, and width of the pulse can be varied. In this work we have used a pulse of 5 μs width, which determines the temporal resolution of the spectroscopic measurements.

The triggering of the pulse generator and the digital oscilloscope is achieved by the signal of the photomultiplier PM2 that detects the lamp light. The temporal evolution of this flashlight can be monitored on a oscilloscope.

The scheme of the lamp can be seen in Fig. 2. Rough-

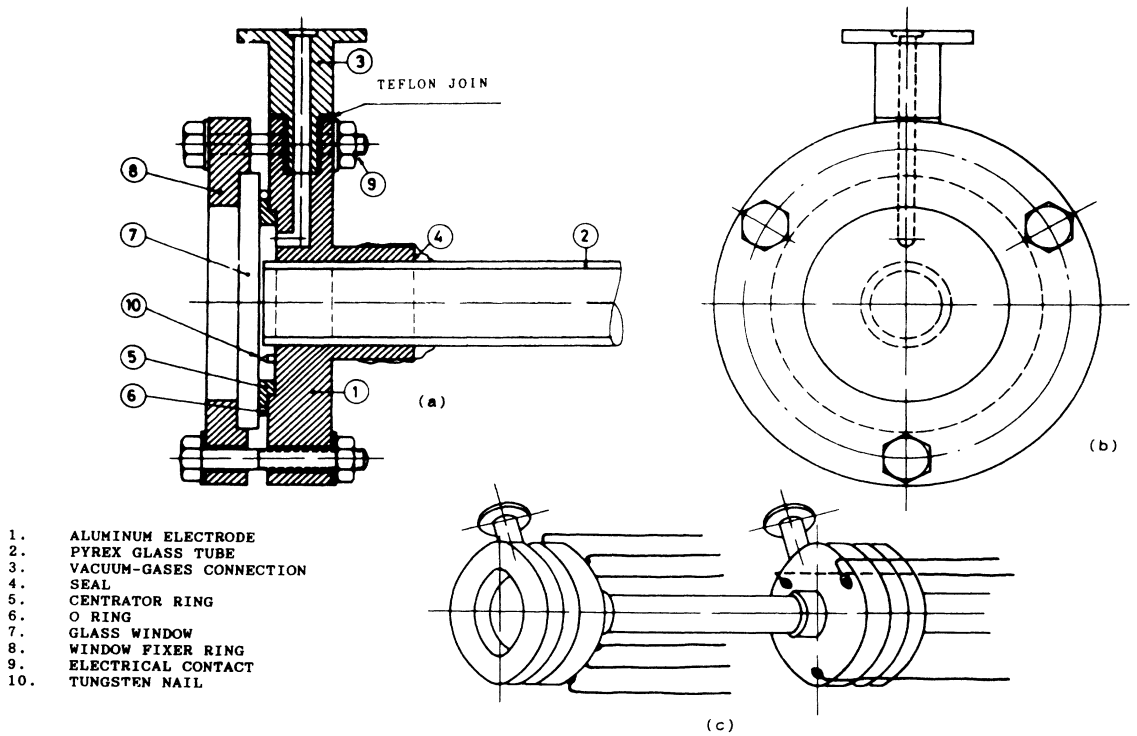

FIG. 2. Discharge lamp.

ly, it consists of a Pyrex glass tube of 15 cm length and 2 cm inner diameter. Two annular pieces of aluminum are glued to the ends and work as electrodes. On the wall is an o ring and on it the glass window. The lamp is closed by a piece of aluminum. The glass tube extends beyond the electrodes, to hide as much as possible the areas near them. This prevents the materials coming from the electrodes during the discharge from reaching the measurement zone. In addition, in these places boundary layers are formed, and their influence is not well known. The electrodes are properly sealed to the tube. The electrical wires were attached symmetrically to the electrodes in order to homogenize the magnetic fields which could have some influence on the plasma. The lamp is connected to the vacuum and gas systems by standard connections placed on the electrodes. The excitation unit has also been designed and constructed in this laboratory. Further details about it can be seen elsewhere.[5]

A typical interferometric record to the wavelength 514.5 nm, already corrected for electrical and luminous background, can be seen in Fig. 3. The main problem of the process of these interference patterns is that, due to their high temporal frequency, it is not possible to use any of the common methods to establish the sign of the phase variation (finite fringe system[6]). Fortunately, in almost all the interference patterns, it was possible to distinguish a point, as the one marked with an arrow in Fig. 3, that allows us to assume, according to the refractivity model, that this is the moment in which the phase variation changes its sign. This assumption has been confirmed by the reproducibility of the results. It is necessary to remark that, in our experiment, it has been possible to record the evolution before the point of maximum electronic density. This is not very easy to find in the literature.

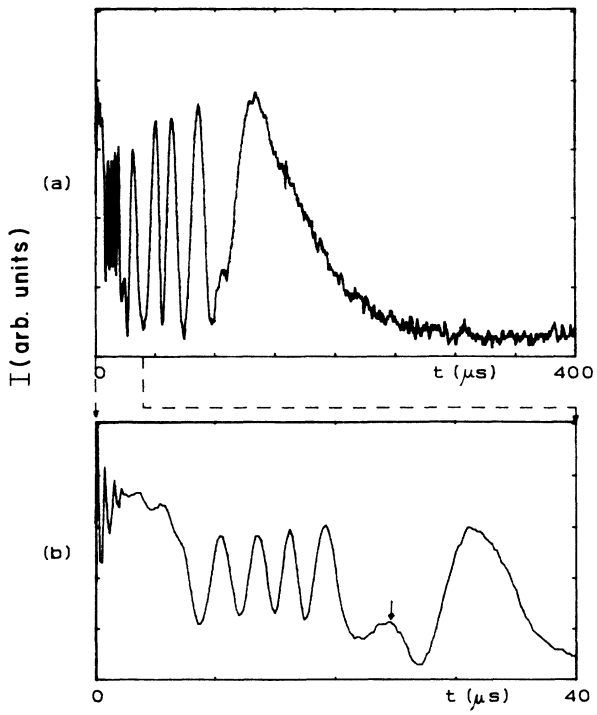

FIG. 3. Typical interferometric record for the wavelength 514.5 nm. The arrow points out the instant of minimum refractivity.

It is also important to point out the contrast losses that appear in the first instant of the plasma creation. Our previous analysis[7] shows that these losses are due to modifications of the wave-front shape, making it not a plane wave, due to radial gradients of the refractive index. This modification would result in the interference state not being constant along the beam, with the resulting contrast loss. This contrast was normalized applying a proportional factor to all the points situated between each maximum and minimum.

We have taken the final part of the interference pattern as the phase origin, when this seems to have reached a stable interference state. This is due to the fact that, with the triggering of our measurement system by lamp light, we do not have records of the previous instants to the plasma flash. The uncertainty in the phase origin is about 0.8%. In this way, we rebuild a harmonic function of temporal variable frequency, from which it is possible to get the phase difference between the interference beams. From these phase differences, it is possible to finally get the total refractivity of the plasma on the assumption that this is the only reason for the different phase changes. This will be discussed later.

In order to obtain the total refractivity of the plasma, we have to take into account that the phase difference obtained from the interferometer is the difference between both the plasma and the neutral helium states at the pressure and temperature of feeding of the lamp (11 mbar and 22 °C):

$$(n-1)_{\text{expt}}=(n-1)_{\text{plasma}}-(n-1)_{\text{initial}}$$

where $(n-1)_{\text{expt}}$ can be directly obtained from the recorded interference patterns:

$$\phi=(2\pi/\lambda)2l(n-1)_{\text{expt}}$$

where l is the length of the plasma column. In our case we have taken this value equal to 15.5 cm, which is the distance between windows. We do not need to consider the existence of boundary layers due to the special design of our lamp. In addition, the estimated width of these layers is very small.[8] It is important to add that the main error source in the determination of the refractivity and so, in the electronic density, comes from this fact.

The refractivity of the helium gas was determined with the same Twyman-Green interferometer, by analyzing the optical path variation between both arms as a function of the filling pressure of the lamp. For 22 °C temperature and 11 mbar pressure, the value of the refractivity is 3.61×10^{-7} with 2% estimated error. This measurement was done only for the wavelength 632.8 nm because there is no dispersion inside the range that we use.[4] The total refractivity of the plasma, in this way, is related to the experimental value by

$$(n-1)_{\text{plasma}}=(n-1)_{\text{expt}}+3.61\times10^{-7}\ .$$

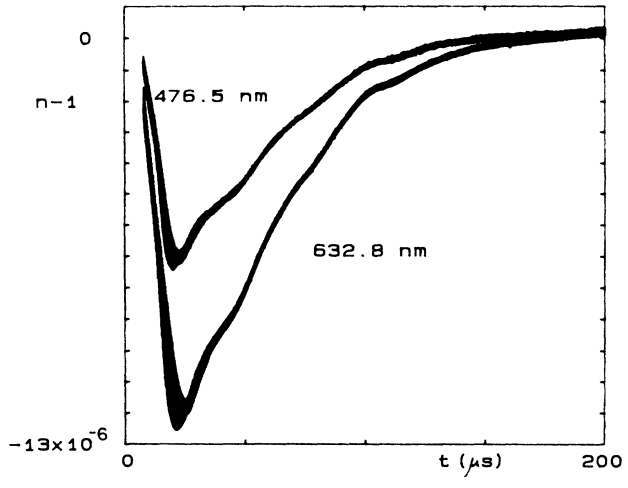

FIG. 4. Plasma refractivity for the two extreme wavelengths in this experiment (476.5 nm, in the upper curve, 632.8 nm, lower curve). Each one is represented with its standard deviation.

In Fig. 4 there are two examples of the total refractivity of the plasma for the wavelengths 476.5 and 632.8 nm, which are the extremes of the interval that we have used. In the same figure there is also a standard deviation obtained by the statistic made with a sufficient number of shots for each experimental condition. An estimation of this deviation lies between 1% and 4% for the instants after the electronic density has reached its maximum.

We have also made spectroscopic measurements in order to obtain the plasma temperature. For that, we have used the procedure of the ratio of intensities. It was possible to measure simultaneously lines from He I and the only present line of He II (468.6 nm) only at certain times of the life of the plasma. As the determination of the temperature using only He I lines is not very accurate, due to the small differences of energy between the upper levels (about 1 eV), we have developed an alternative method, taking into account the local thermodynamic equilibrium (LTE) equations, using the known temperature values. A further description of this method can be seen elsewhere.[9]

$$N_{\mathrm{He\,II}}=\frac{N_e^2}{2\dfrac{U_{\mathrm{He\,III}}(T)}{U_{\mathrm{He\,II}}(T)}4.8303\times10^{15}T^{3/2}\exp(-\chi_{\mathrm{He\,II}}/k_BT)+N_e},$$

$$N_{\mathrm{He\,I}}=\frac{N_eN_{\mathrm{He\,II}}U_{\mathrm{He\,I}}(T)}{U_{\mathrm{He\,II}}(T)}\frac{1}{4.8303\times10^{15}T^{3/2}\exp(-\chi_{\mathrm{He\,I}}/k_BT)}.$$

All of the data necessary for these calculations can be found elsewhere.[10–12]

In Fig. 5, one can see the temporal evolution of the temperature that we have used. As we have mentioned, we have done spectroscopic measurements to obtain the temperature. The method[9] used allows us to calculate the temperature, not only where it is possible to obtain simultaneously the lines used, but also during the whole

RESULTS

In order to analyze the experimental results, we have followed two types of studies. On one hand, the common technique of determination of electronic density is based on the assumption that the contribution of the rest of the nonelectronic species is constant with wavelength. If we have measurements at several wavelengths, the natural extension of the previous procedure is to perform, for each moment of the plasma life, a fitting like

$$(n-1)_{\mathrm{plasma}}=a\lambda^2+b\ .$$

Taking into account the expression of the plasma refractivity, the a coefficient is related to the electronic density by

$$a=-4.485\times10^{-14}N_e$$

and the b coefficient gives directly the contribution to the refractivity of the rest of the species, if we assume that this contribution is a constant.

On the other hand, if we assume that the plasma is under LTE, it is possible to write the contribution to the refractivity of the rest of the nonelectronic species as follows:

$$(n-1)_\alpha=4.485\times10^{-14}\sum_{\substack{i,k\\ i\neq k}}\frac{f_{ik}\lambda_{ik}^2\lambda^2}{(\lambda^2-\lambda_{ik}^2)}\frac{g_i}{U_\alpha(T)}\times\exp[(-E_i/k_BT)N_\alpha]$$

where g refers to the statistical weight, U is the partition function, α refers to each of the species He I and He II, and the sum is extended not only to resonance lines, but also to all the transitions for which data were available in the literature, for the ground and excited states of each species. The contribution of He III has the same functional dependence on the wavelength that the free electrons have, but is smaller by their respective mass ratios. Thus this contribution was not taken into account. On the other hand, the population of He III was considered when we calculated the population balance due to the high temperatures in our experiments. In this way, we can minimize the difference between experimental and theoretical data as a function of N_e.

The population of both species under LTE is given by

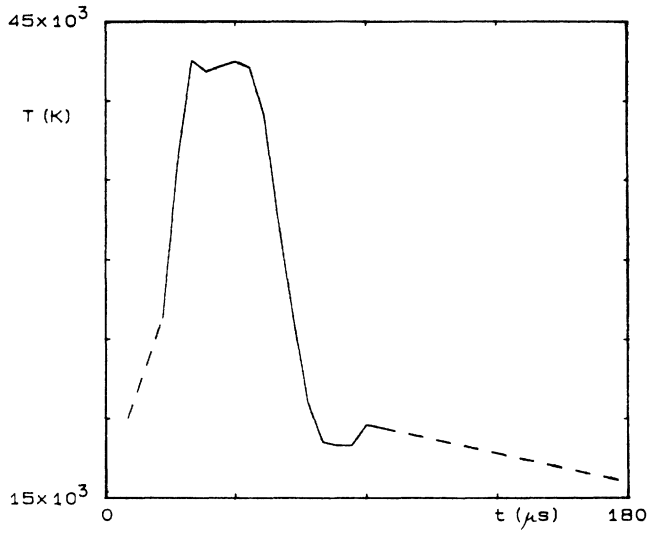

FIG. 5 Evolution of the plasma temperature. The continuous line is the temperature obtained by the mentioned method, the dashed line corresponds to an extrapolation.

of the plasma luminous period. These data are represented by the continuous line in Fig. 5. As we have interferometric data further away from the luminous life, it was necessary to extrapolate the temperature, using the available data; this is the dotted line of Fig. 5. Obviously, the reliability of this last part is less, although it does not affect the process significantly due to the slight dependence on the temperature of the refractivity.

In Fig. 6, we have represented the electronic densities obtained by both methods and in Fig. 7, their percent difference. It can be seen that the agreement is very good during approximately the whole plasma luminous period. This agreement is not very satisfactory at the very beginning of the plasma life, but at these times the measurements are less reproducible. These times correspond to the rise of electronic density. The agreement is also not so good at the end.

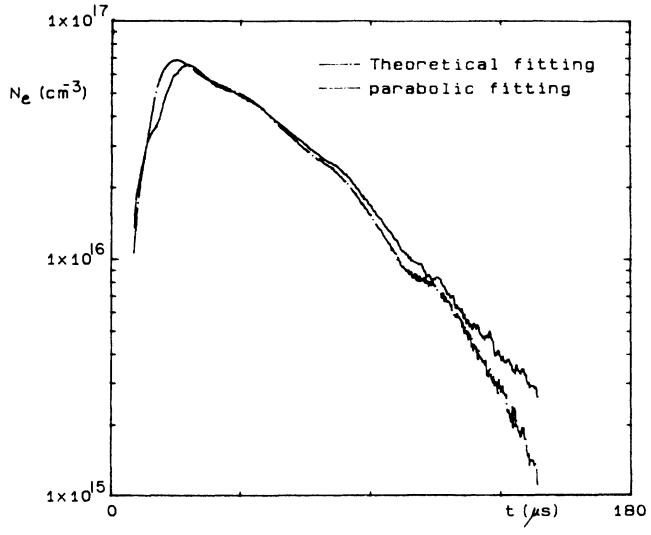

FIG. 6. Electronic density obtained by both methods.

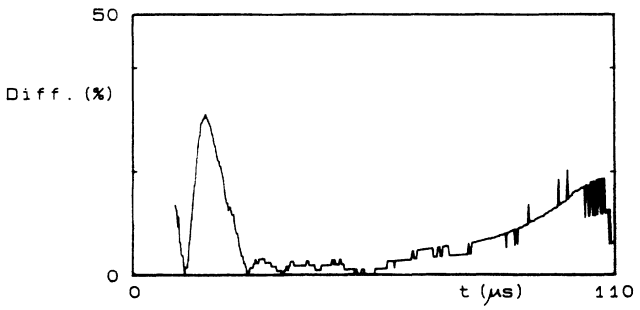

FIG. 7. Discrepancy between the electronic densities obtained by both methods.

One can see in Fig. 8 the comparison of the contribution of the nonelectronic species to refractivity obtained by both methods. In the case of the parabolic fitting we have added its deviation. The result for the parabolic fitting is shown for the wavelength 476.5 nm, even though, with this scale, the results for other wavelengths will be indistinguishable. As can also be seen, the theoretical result does not overlap with the parabolic fitting in most of the figure, though the difference is very small.

With the aim of being more precise, we have considered different contributions that would explain these already very small discrepancies. For example, we have calculated the contribution to the refractivity of certain spectral lines belonging to possible impurities of the gas, in particular nitrogen and oxygen. We have proved that its influence will be several orders of magnitude less than necessary. Other possible causes, such as cathode effects or the escape of particles, are not likely. Finally, in a

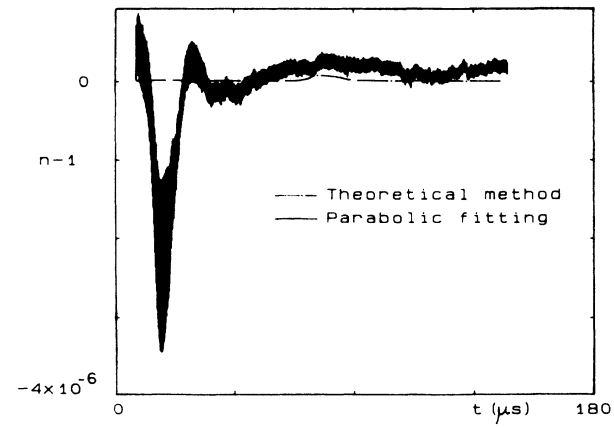

FIG. 8. Contribution to the refractivity of the nonelectronic species. The one obtained by the parabolic fitting is represented with its standard deviation. The one obtained by the theoretical fitting corresponds to the wavelength 476.5 nm.

different work we have analyzed the influence of the windows.[3] We have concluded that the windows suffer mechanical and thermal perturbations. However, we think that these perturbations do not disturb the measurement of the refractivity along the lamp axis, at least in a lamp such as ours. In the case of the heating and the following cooling, this has no effect if the phase origin is taken, as we do, at the end of the interference pattern, due to the differences of temporal scales in both phenomena. If we took this origin at any instant before the lamp excitation, this phenomenon would disturb the measurement.

As one of the conclusions of this work, we will say that with an accuracy of about 5% and for most instants of the plasma life (corresponding to the decay of the electronic density), the parabolic fitting method gives an electronic density which is in good agreement with theoretical calculations based on LTE. In addition to this, if another cause of perturbation of the measurement exists, as seems to be likely from Fig. 8, it would be better to take it into account this contribution to the refractivity as a constant with the wavelength than not to take it into account. Thus the determination of the electronic density by the parabolic fitting method will be more precise than from complicated theoretical calculations.

ACKNOWLEDGMENTS

We thank Dr. M. Quintanilla (Universidad de Zaragoza) and Dr. A. Czernikowski (Université d'Orleans) for their useful suggestions on these problems. We thank, also, the Dirección General de Investigación Científica y Técnica (Ministerio de Educasión y Ciencia) of Spain for its financial support under Contract No. PB86/0331.

[1]N. Konjevic and W. L. Wiese, J. Phys. Chem. Ref. Data **5**, 2 (1976).

[2]R. A. Alpher and D. R. White in *Plasma Diagnostic Techniques,* edited by R. H. Huddlestone and S. L. Leonard (Academic, New York, 1965).

[3]R. A. Alpher and D. R. White, Phys. Fluids **2**, 162 (1959).

[4]M. Born and E. Wolf, *Principles of Optics* (Pergamon, Oxford, 1975).

[5]I. González, S. Mar, and V. Cardeñoso, Atti Fond. "Giorgio Ronchi" **XLI**, 501 (1986).

[6]N. Abramson, *The Making and Evaluation of Holograms* (Academic, New York, 1981).

[7]Ma. I. de la Rosa, Ph.D. thesis, Universidad de Valadolid (1989).

[8]J. D. Cobine, *Gaseous Conductors* (Dover, New York, 1958).

[9]M. I. González, M. C. Pérez, M. I. de la Rosa, and S. Mar, Jpn. J. Appl. Phys. **29**, 1189 (1990).

[10]J. Reader, C. H. Corliss, W. L. Wiese, and G. A. Martini, *Wavelengths and Transition Probabilities for Atoms and Atomic Ions* (National Bureau of Standards, Washington, D.C. 1980).

[11]W. L. Wiese, M. W. Smith, and B. M. Glennon, *Atomic Transition Probabilities* (National Bureau of Standards, Washington, D.C. 1966), Vol. 1.

[12]A. R. Striganov and N. S. Sventitskii, *Tables of Spectral Lines of Neutral and Ionized Atoms* (Plenum, New York, 1968).

[13]Ma. I. de la Rosa, Ma. C. Pérez, A. M. de Frutos, and S. Mar, Appl. Opt. (to be published).